Testing of Frozen Turbulence Hypothesis for Wind Turbine Applications with a Scanning LIDAR System

Schlipf, D.; Trabucchi, D.; Bischoff, O.; Hofsäss, M.; Mann, Jakob; Mikkelsen, Torben; Rettenmeier, A.; Trujillo, J.; Kühn, M.

Published in:
Detaled Program

Publication date:
2010

Document Version
Publisher's PDF, also known as Version of record

Testing of Frozen Turbulence Hypothesis for Wind Turbine Applications with a Scanning LIDAR System

D. Schlipf[1], D. Trabucchi[2], O. Bischoff[1], M. Hofsäß[1], J. Mann [3], T. Mikkelsen[3], A. Rettenmeier[1], J.J. Trujillo[1], M. Kühn[1]

[1] *Endowed Chair of Wind Energy at Universität Stuttgart, Germany*
[2] *Politecnico di Milano, Italy*
[3] *Risø, Technical University of Denmark, Denmark*

ABSTRACT

Taylor's frozen turbulence hypothesis is tested in its applicability for wind turbine applications. In this research full field measurements are performed at a test site for multi-megawatt wind turbines by means of a pulsed LIDAR with a scanning device. The system is installed at the top of the nacelle of a $5\,\mathrm{MW}$ wind turbine. It provides simultaneous wind speed, with a maximum sampling rate of $5\,\mathrm{Hz}$, at different stations parallel to the mean wind. Measurements in a range between 0.4 and 1.6 rotor diameter are performed following several two and three dimensional trajectories. The spectral characteristics of measurements taken simultaneously at different separation distances are studied. The scanning strategy which maximizes the wavenumber region where results are consistent with Taylor's hypothesis is assessed. The best results are achieved by a horizontal sliding trajectory with valid wavenumbers up to $0.125\,\mathrm{rad/m}$.

1 INTRODUCTION

The study of atmospheric turbulence covers a wide range of topics which arises interest in several fields of both science and engineering. This research deals with the investigation of Taylor's hypothesis over an open field in the inflow of a $5\,\mathrm{MW}$ wind turbine. The assumption states that, under certain conditions, the turbulent structures move as frozen entities transported by the mean wind. This allows deriving the spatial pattern of turbulence from its temporal description. The hypothesis of frozen turbulence is relevant for wind energy because it provides a simple and robust model to simulate the flow of a wind field. It simplifies the use of remote wind measurements for predictive control and the study of the wind turbine wake.
The upstream flow in front of a wind turbine is not fully conform with the assumptions required by Taylor's hypothesis. However in regards to the intended application, the validity of the frozen turbulence hypothesis has to be assessed. This research is intended to detect the eddies' scales and the correlated frequency and wavenumber range where Taylor's hypothesis best fits the real turbulence behavior. In order to achieve this purpose, a system composed by a pulsed LIDAR with an integrated scanning device [1] was set on the nacelle of a 5MW wind turbine and used to check the existence of certain scales of turbulent structures which could be considered as frozen. A pulsed LIDAR system gives the advantage of measuring simultaneously the line of sight wind speed at different distances and facilitates the study of Taylor's hypothesis by means of a cross-spectral analysis.

2 TAYLOR'S HYPOTHESIS

In a turbulent air flow with a mean speed $\overline{u_i}$, the turbulent oscillations u_i' can be defined as:

$$u_i' = u_i - \overline{u_i} \quad i = 1,2,3 \tag{1}$$

where u_i is the air velocity and *i*= 1, 2, 3 indicates respectively the longitudinal, lateral and vertical direction. Most commonly the flow is assumed to be isotropic. In such cases the longitudinal component is enough to represent the whole field of turbulence. As the white light can be imagined like the superposition of waves characterized by all the different wavelengths, it is possible to figure turbulence like the superposition of several structures, each one characterized by a wavelength vector λ which describes its spatial distribution. In the case of turbulence, the larger structures are known as eddies, and, according to Taylor's hypothesis [2] they do not evolve and are convected by the average wind flow. A consequence of this can be seen considering the following example taken from [3] and represented in Figure 1.
An eddy with a diameter of 100m has a temperature difference of 5ºC between the front and back side. The same eddy, 10 seconds later, is blown downwind at a wind speed of 10 m/s. The relative equation which describes this behavior is:

$$\frac{dT}{dt} = \frac{\partial T}{\partial t} + \overline{u}\frac{\partial T}{\partial x} = 0 \quad \Rightarrow \quad \frac{\partial T}{\partial t} = -\overline{u}\frac{\partial T}{\partial x}, \tag{2}$$

where T is the temperature, t the time, x the wind direction and $\overline{u}$ the mean wind speed. The same concept can be extended in all directions to other variables that characterize the flow:

$$\frac{\partial \xi}{\partial t} = -\left(\overline{u}\frac{\partial \xi}{\partial x} + \overline{v}\frac{\partial \xi}{\partial y} + \overline{w}\frac{\partial \xi}{\partial z}\right), \tag{3}$$

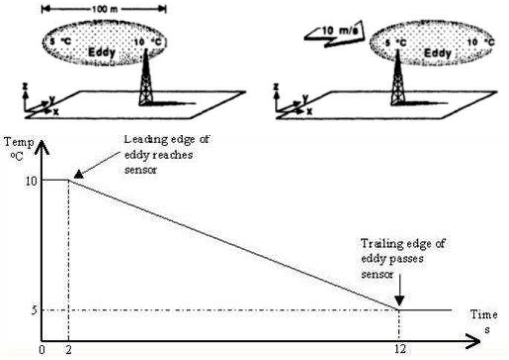

Figure 1. *Taylor's hypothesis example [3]*

where ξ stands for a general variable of the flow and $\overline{u}$, $\overline{v}$, $\overline{w}$ for the average wind components in x, y, z direction, respectively. A simple test of Taylor's hypothesis validity is the comparison of two data series of the longitudinal turbulence u'_A and u'_B, taken at two fixed points A and B along the wind flow. In such a case, the two measures are expected to be equal and to be relatively shifted by the time required for the wind to cover the separation distance between A and B. Since it evaluates the similarity of two series in function of their relative lag τ, the correlation coefficient is a suitable function for the intended purpose. It is the normalization of the correlation function $R(\tau)$ by means of the covariance σ^2_{AB} between u'_A and u'_B, that varies in the interval [-1,1] approaching 1 as much as two series are correlated and reaches its maximum at the lag that synchronizes best the two series and therefore corresponds to their relative shift.

$$\rho_{AB}(\tau) = \frac{R(\tau)}{\sigma^2_{AB}} = \frac{E[u'_A(t)u'_B(t+\tau)]}{E[u'_B(t)u'_A(t)]} \tag{4}$$

A deeper characterization can be achieved by means of the spectral analysis, in particular with the coherence $\gamma^2_{AB}(f)$ and the phase $\phi(f)$ of the cross energy spectra density $S_{AB}(f)$:

$$\begin{aligned} S_{AB}(f) &= \int_{-\infty}^{+\infty} R_{AB}(\tau) e^{-i^* 2\pi f \tau} dt \\ &= |S_{AB}(f)| e^{-i^* \phi_{AB}(f)} \\ \gamma^2_{AB}(f) &= \frac{|S_{AB}(f)|^2}{S_{AA}(f) S_{BB}(f)} \\ \phi(f) &= \angle S_{AB}(f). \end{aligned} \tag{5}$$

To compute the described functions, it was chosen to perform the Welch periodogram, in order to minimize the statistical errors. According to Taylor's hypothesis, $\gamma(f)^2$ should be one for all frequencies, while $\phi(f)$ should be proportional to the delay between u_A and u_B:

$$\frac{d\phi(f)}{df} = 2\pi\tau_0 = 2\pi\frac{x_{AB}}{\overline{u}} \tag{6}$$

3 NACELLE LIDAR MEASUREMENTS

The experimental tests analyzed in this research involved a pulsed LIDAR enhanced with a sophisticated scanning device developed by the Endowed Chair of Wind Energy (SWE). The whole system is mounted at a height of about 102 m, on the nacelle of a $5\,\mathrm{MW}$ wind turbine whose rotor diameter D measures $116\,\mathrm{m}$. The turbulence oscillations were first recorded along a fixed direction (staring mode) at five different Focus Distances (FD) in the range of 0.4-1.2 D. In this way, the wind speed in a single point might not provide an accurate description of the whole flow which passes through the turbine rotor. Because of this reason, measurements were performed not only in staring mode, but also following different two and three dimensional trajectories centered on the turbine axis (see Figure 2), with reference dimensions comparable with the rotor diameter D, varying the distances and their separation (see Table 1).

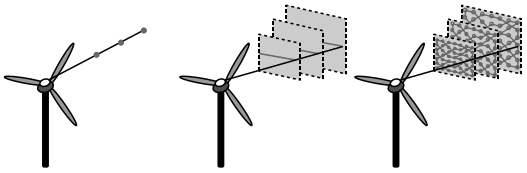

Figure 2. *Trajectories sketch*

id	Trajectory	Points h. x v	Proj. at $1D$ [D] width x height	Time [s]	Range [D] From	Step	To
A	Staring	1x1	0.00x0.00	0.20	0.40	0.20	1.40
B	Sliding	5x1	0.75x0.00	1.60	0.50	0.25	1.50
C	Sliding	9x1	0.75x0.00	3.20	0.60	0.20	1.40
D	Lissajous2Grid	4x3	0.80x0.15	2.08	0.40	0.20	1.20
E	Lissajous2Grid	6x5	0.50x0.50	5.40	0.40	0.20	1.20
F	Lissajous2Grid	7x7	0.75x0.75	8.39	0.50	0.25	1.50
G	Lissajous2Grid	7x7	0.75x0.75	8.29	0.40	0.20	1.20

Table 1. *Description of the measuring campaigns.*

4 DATA ANALISIS AND RESULTS

The data series are first separated from low quality records, which are mainly the consequence of lack of particles in the atmosphere or impact of the laser beam with the rotating blades. Those data can be filtered with the help of the Carrier-to-Noise-Ratio (CNR). For exemple an inpact with the rotating blades usually results in a Gaussian distribution below -17dB

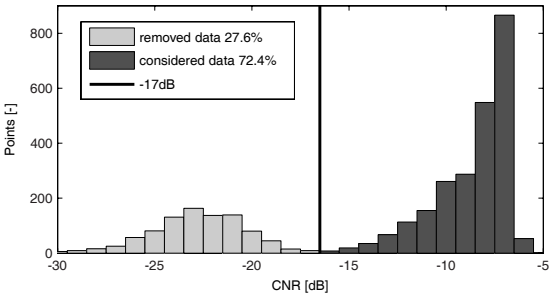

Figure 3. *Typical 10min-histogram of CNR values.*

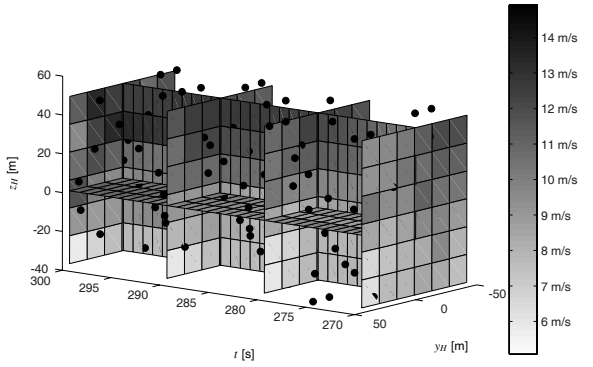

Figure 4. *Example of 3D interpolation of filtered measurements. The dots mark the focus points.*

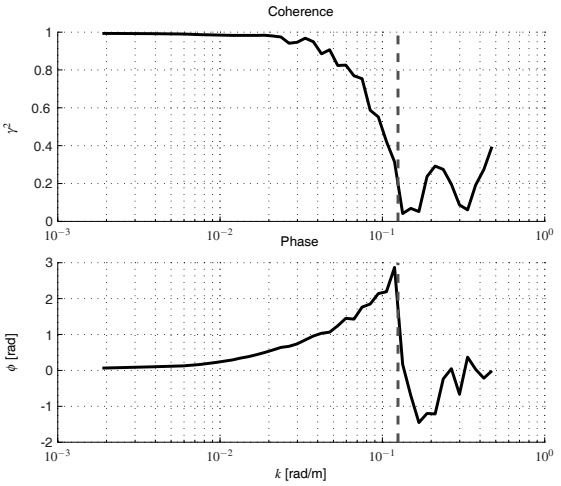

Figure 5. *Coherence and phase between the two closest FD of scanning trajectory-C (black) and maximum valid wavenumber $\hat{k}$ (dark gray).*

(see Figure 3). Then, the remaining data is interpolated on a uniform time grid (see Figure 4). For one/two dimensional measurements, also a space interpolation is required. In both cases, the grids are chosen in order to have the nodes as close as possible to the measured points. The next steps first consist in the classification of the data according to the mean wind speed and the turbulence intensity, secondly in coupling the simultaneous data series in order to perform the cross-analysis on all the possible pairs.
Considering the frequency region limited by f_i such that $\gamma(f_1)^2 = 0.9$, $\gamma(f_2)^2 = 0.8$ and $\gamma(f_3)^2 = 0.7$, it is possible to transform the frequency to the wavenumber $k = \frac{1}{\lambda}$ using the longitudinal average wind speed $\overline{u}$:

$$k_i = 2\pi \frac{f}{\overline{u}} \tag{7}$$

Since the best result was achieved between the two closest FD of scanning trajectory-C (see Figure 5), this one was chosen for a first study of the phase. Using the relation displayed in (5) the theoretical delay τ_0 was computed from the separation distance x_{AB} and the mean wind speed $\overline{u}$. Then it was compared with the one evaluated from the phase ϕ. In order to

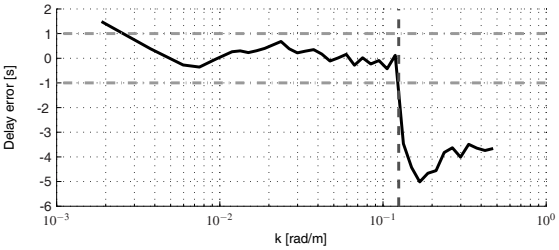

Figure 6. *Error of the time delay estimation for the phase between the two closest FD of scanning trajectory-C(black), tolerance (light gray) and maximum valid wavenumber $\hat{k}$ (dark gray).*

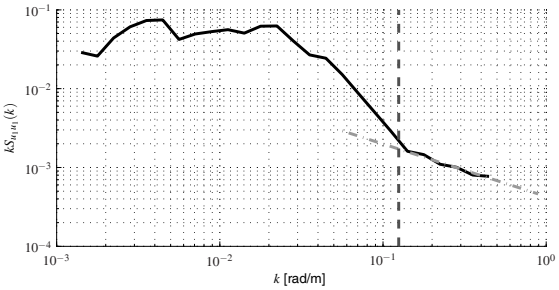

Figure 7. *Energy spectra for the closest FD of scanning trajectory-C(black), Kolmogorov cascade theory (light gray) and maximum valid wavenumber $\hat{k}$ (dark gray).*

find a band of confidence of Taylor's hypothesis also for the phase, the limit of the absolute difference between the expected and the measured delay was set to $1\,\mathrm{s}$. The error shown in Figure 6 is within the tolerated range up to $\hat{k}$= 0.125 rad/m. It is interesting to compare the results with the energy spectra kS_{xx}. According to Kolmogorov cascade theory [4], in turbulent flows the biggest eddies take energy from the main stream and through an instability process transfer the energy to smaller eddies until these turbulent structures are no more unstable and vanish converted in heat. The instability process lies in the inertial range, which is the band where the slope of the energy spectra density S_{xx} is $k^{-5/3}$. Because of the energy transfer, the eddies evolve and, therefore, in this range Taylor's hypothesis can not be considered applicable. In Figure 7, kS_{xx} is represented as well as the theoretical slope, which in this case is $k^{-5/3} \times k = k^{-2/3}$. It can be noticed that the inertial range begins exactly where the delay error overtakes the tolerance limit which is the same wavenumber $\hat{k}$ at which coherence is near to zero.
If the measurements are used e.g. for look-ahead control [5], the data has to be filtered to avoid incorrect control action because of wrong prediction, depending on the wavenumber $\hat{k}$ and the mean wind $\overline{u}$.
In Figure 8 the considered signals was filtered (Butterworth, 2nd order) with the corresponding Cut-off-frequency $f_f = \frac{\hat{k}\overline{u}}{2\pi} = 0.126\,\mathrm{Hz}$.

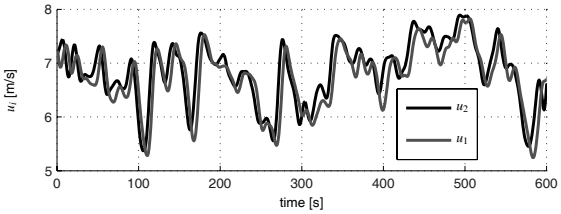

Figure 8. *Filtered Signals.*

5 CONCLUSION

The experimental results of this research confirm Taylor's frozen turbulence hypothesis concerning eddies within length scales that are relevant for multi-MW wind turbines. Based on the coherence, the hypothesis could be found valid with a 90% accuracy for eddy length scales in the order of two rotor diameters.
Furthermore, considering the phase, the beginning of the inertial range can be considered as the limit of the frozen turbulence model confidence band which was found at about $0.125\,\mathrm{rad/m}$.

ACKNOWLEDGEMENT

This work is part of the research project "Further development of LIDAR measurements for the offshore test field" which is funded by the German Environment Ministry under the code number 0327642.

REFERENCES

[1] Rettenmeier, A., Bischoff, O., Hofsäss, M., Schlipf, D., Trujillo, J. J., and Kühn, M., "Wind field analyses using a nacelle-based LIDAR system," *Proc. EWEC*, 2010.

[2] Taylor, G., "The spectrum of turbulence," *Proceedings of the Royal Society of London*, 1938.

[3] Stull, R., *An introduction to boundary layer meteorology*, Kluwer Academic Publishers, 1989.

[4] Pope, S., *Turbulent Flows*, Cambridge University Press, 2000.

[5] Schlipf, D., Schuler, S., Grau, P., Allgöwer, F., and Kühn, M., "Look-Ahead Cyclic Pitch Control Using LIDAR," *Proc. Science of Making Torque from Wind*, 2010.